Pharmacological Research 97 (2015) 27–39

Contents lists available at ScienceDirect

Pharmacological Research

journal homepage: www.elsevier.com/locate/yphrs

Classical and atypical agonists activate M_1 muscarinic acetylcholine receptors through common mechanisms

Alena Randáková [a], Eva Dolejší [a], Vladimír Rudajev [a], Pavel Zimčík [a], Vladimír Doležal [a], Esam E. El-Fakahany [b], Jan Jakubík [a,*]

[a] Institute of Physiology Czech Academy of Sciences, v.v.i., 142 20 Prague, Czech Republic
[b] Department of Experimental and Clinical Pharmacology, University of Minnesota College of Pharmacy, Minneapolis, MN 55455, USA

ARTICLE INFO

Article history:
Received 17 February 2015
Received in revised form 3 April 2015
Accepted 3 April 2015
Available online 13 April 2015

Keywords:
Muscarinic acetylcholine receptors
Atypical agonists
Xanomeline
Activation mechanism

Chemical compounds studied in this article:
Carbachol (PubChem CID: 5831)
N-desmethylclozapine (PubChem CID: 2820)
Oxotremorine (PubChem CID: 4630)
Xanomeline (PubChem CID: 60809)

ABSTRACT

We mutated key amino acids of the human variant of the M_1 muscarinic receptor that target ligand binding, receptor activation, and receptor-G protein interaction. We compared the effects of these mutations on the action of two atypical M_1 functionally preferring agonists (N-desmethylclozapine and xanomeline) and two classical non-selective orthosteric agonists (carbachol and oxotremorine). Mutations of D105 in the orthosteric binding site and mutation of D99 located out of the orthosteric binding site decreased affinity of all tested agonists that was translated as a decrease in potency in accumulation of inositol phosphates and intracellular calcium mobilization. Mutation of D105 decreased the potency of the atypical agonist xanomeline more than that of the classical agonists carbachol and oxotremorine. Mutation of the residues involved in receptor activation (D71) and coupling to G-proteins (R123) completely abolished the functional responses to both classical and atypical agonists. Our data show that both classical and atypical agonists activate hM_1 receptors by the same molecular switch that involves D71 in the second transmembrane helix. The principal difference among the studied agonists is rather in the way they interact with D105 in the orthosteric binding site. Furthermore, our data demonstrate a key role of D105 in xanomeline wash-resistant binding and persistent activation of hM_1 by wash-resistant xanomeline.

1. Introduction

Muscarinic acetylcholine receptors are abundantly expressed in the central and peripheral nervous system and innervated tissues. They serve a wide array of physiological roles ranging from vegetative functions up to cognition [1]. Damage of cerebral cholinergic transmission either due to injury, neurodegeneration, toxins or aging manifests itself as neurological or psychiatric diseases including Alzheimer's disease [2,3] and schizophrenia [4]. Thus muscarinic receptors represent an obvious target for pharmacological interventions. Muscarinic ligands that are selective for certain subtypes of muscarinic receptors are needed for this purpose. However, all five muscarinic receptor subtypes share high sequence homology, especially in the orthosteric binding site. Current crystallographic structures of M_2 and M_3 receptors [5,6] show that homology in the secondary and tertiary structure extends even beyond the orthosteric binding site. This high homology hindered the discovery of ligands that bind selectively to specific receptor subtypes. However, it has recently been discovered that certain agonists that do not differentiate in their binding affinity to various muscarinic receptors display functional selectivity.

Xanomeline was among the first agonists of this class [7] followed by AC-42 (4-[3-(4-butylpiperidin-1-yl)-propyl]-7-fluoro-4*H*-benzo[1,4]oxazin-3-one) [8]. Subsequently, new M_1 selective agonists based on TBPB ([1-(1–2-methylbenzyl)-1,4-bipiperidin-4-yl)-1*H*-benzo[*d*]imidazol-2(3*H*)-one]) [9] as well as ones structurally related to AC-42 [10] and xanomeline [11,12] were identified. Interestingly, all these M_1 selective compounds display deviations from competitive binding and can be considered atypical agonists.

A particular feature of xanomeline binding to muscarinic receptors is its resistance to extensive washing [7]. Wash-resistant xanomeline affects binding of orthosteric ligands both competitively and allosterically [13]. Xanomeline may thus be labeled as a dual-steric or bitopic agonist. Its functional but not binding

Abbreviations: CHO, Chinese hamster ovary; KHB, Krebs-HEPES buffer; NDMC, N-desmethylclozapine; NMS, N-methylscopolamine; TCA, trichloracetic acid.

* Corresponding author at: Institute of Physiology CAS, v.v.i., Vídeňská 1083, 142 20 Prague, Czech Republic. Tel.: +420 2 4106 2620; fax: +420 2 4106 2488.
E-mail address: jakubik@biomed.cas.cz (J. Jakubík).

http://dx.doi.org/10.1016/j.phrs.2015.04.002

selectivity makes it an attractive ligand for research of the mechanisms of receptor activation. During the past decade, the mechanisms of xanomeline binding have been partly identified [13] but the conundrum of xanomeline functional selectivity has yet to be satisfactorily untangled, especially in regard to its long-term antagonism of M_5 receptors [14] and prolonged activation of the remaining four muscarinic receptor subtypes that is preferential to M_1 and M_4 receptors [15]. Differential kinetics of receptor activation [16,17], the ability of xanomeline to induce specific conformations of muscarinic receptors [18,19] and multiple activation switches in muscarinic receptors specific for allosteric ligands [20] may explain its functional selectivity. Another interesting atypical M_1 preferential muscarinic agonist is N-desmethylclozapine (NDMC), a pharmacologically active metabolite of clozapine, a drug used in treatment of schizophrenia. Allosteric properties and unique activation mode by NDMC have been described [21,22].

Besides its pure scientific interest, understanding the molecular mechanisms of functional agonist selectivity is key to knowledge-based development of functionally selective muscarinic agonists with potential therapeutic use. To address this question we mutated key amino acids of the human variant of the M_1 muscarinic receptor that participate in ligand binding, receptor activation, and receptor-G protein interaction and compared how these mutations affect signal transduction by two atypical M_1-preferring agonists (NDMC and xanomeline) and two classical non-selective orthosteric agonists (carbachol and oxotremorine).

2. Materials and methods

2.1. Receptor mutagenesis and generation of cell lines

New stable CHO cells lines expressing wild-type and mutant M_1 receptors have been prepared. The mammalian expression vector pcDNA3.1 (Invitrogen) containing the coding sequence of the human variant of M_1 mAChR subtype was obtained from Missouri S&T cDNA Resource Center (Rolla, MO, USA). This plasmid was used to generate hM_1 mAChR sequences with the desired amino acid substitution using Quick Change II Site-directed Mutagenesis Kit (Stratagene). Chinese hamster ovary (CHO-K1) cells were transfected with either original hM_1-pcDNA or mutated plasmid using Lipofectamine 2000 (Invitrogen). Subconfluent cells were washed with phosphate-buffered saline and Opti-MEM (Life Technologies) containing Lipofectamine at final concentration of 5 μL/mL and plasmid DNA at final concentration of 1 μg/mL was applied to the cells for 6 h. After 48 h cells were diluted 10 times by subculturing and geneticin (Life Technologies) was added to the cultivation medium to a final concentration of 1000 ng/mL. Expression of new constructs was checked by reverse transcription quantitative PCR. Mediator RNA was isolated from CHO cell lines using TriPure Isolation Reagent (Roche). Reverse transcription was done using M-MLV Reverse Transcriptase (Promega), Oligo (dT) anchored primers and quantified using LightCycler® 480 SYBR Green I Master in LightCycler® 480 Instrument II system (Roche) and analyzed by LightCycler® 480 Software 1.5.0. Cell lines expressing wild-type (wt) or mutated M_1 receptors with comparable receptor expression level were used for functional experiments. The numbering of residues of the hM_1 receptor is used in this manuscript.

2.2. Cell culture and membrane preparation

Chinese hamster ovary cells stably transfected with wild-type (wt) human M_1 or mutated receptors were grown to confluence in 75 cm^2 flasks in Dulbecco's modified Eagle's medium supplemented with 10% fetal bovine serum. Two million cells were subcultured to 100-mm Petri dishes. Medium was supplemented with 5 mM sodium butyrate for the last 24 h of cultivation to increase receptor expression. Cells were washed with phosphate-buffered saline and manually harvested on day 5 after subculture. Cells were centrifuged for 3 min at 250 × *g*. Pellet was suspended in 10 mL of ice cold homogenization medium (100 mM NaCl, 20 mM Na-HEPES, 10 mM EDTA, pH 7.4) and homogenized on ice by two 30 s strokes using Polytron homogenizer (Ultra-Turrax; Janke & Kunkel GmbH & Co. KG, IKA-Labortechnik, Staufen, Germany) with a 30-s pause between strokes. Cell homogenates were centrifuged for 5 min at 1000 × *g*. The supernatant was collected and centrifuged for 30 min at 30,000 × *g*. Pellets were suspended in incubation medium (100 mM NaCl, 10 mM $MgCl_2$, 20 mM Na-HEPES, pH 7.4), left for 30 min at 4 °C, and then centrifuged again for 30 min at 30,000 × *g*. Resulting membrane pellets were kept at −80 °C until assayed.

2.3. Radioligand binding experiments

Membranes (10–30 μg of membrane proteins per sample) were incubated in 96-well plates for 3 h at 30 °C in 400 μL of incubation medium. In saturation experiments of binding of [^{3}H]NMS six concentrations of the radioligand (ranging from 63 to 2000 pM) were used. Alternatively, saturation binding was measured using [^{3}H]QNB in concentrations ranging from 12.5 to 400 pM at the M_1 wt and ranging from 1.25 to 40 nM at the D105N mutant. Agonist binding was determined in competition experiments with 1 nM [^{3}H]NMS. Nonspecific binding was determined in the presence of 10 μM atropine. In case of [^{3}H]QNB saturation binding at D105N mutant the concentration of atropine was increased to 40 μM. Incubation was terminated by filtration through Whatman GF/B glass fiber filters (Whatman) using a Brandel harvestor (Brandel, USA). Filters were dried in a microwave oven (3 min, 800 W) then solid scintillator meltilex A was melted on filters (105 °C, 60 s) using a hot plate. The filters were cooled and counted in a Wallac Microbeta scintillation counter (Wallac, Finland).

To determine xanomeline wash-resistant binding prior to incubation with [^{3}H]NMS membranes were either sham treated or treated with xanomeline as follows. Membranes were resuspended in incubation buffer (1 mg of proteins per mL) supplemented with xanomeline in final concentrations ranging from 100 nM to 1 mM and incubated for 20 min at 37 °C. Then membranes were washed 3-times in 10-fold volume of incubation buffer by recentrifugation (30 min at 30,000 × *g*). Membranes were then resuspended in 10-fold volume of incubation buffer and incubated for 1 h and again washed 3-times by recentrifugation.

2.4. Accumulation of inositol phosphates (IP_X)

Accumulation of inositol phosphates (IP_X) was assayed in attached cells grown in 24-well plates. Cells were prelabeled over night by 100 nM [^{3}H]myo-inositol (ARC, USA) in 0.3 mL of DMEM at 37 °C. Cells were then washed with fresh medium and preincubated in 0.4 mL of DMEM containing 10 mM LiCl for 15 min at 37 °C. The indicated concentrations of agonists were added and samples were incubated for additional 20 min in a final incubation volume of 0.5 mL. The reaction was stopped by adding 0.2 mL of cold 20% trichloroacetic acid (TCA). TCA precipitates were dissolved in 0.2 mL of 1 M NaOH. Aliquots of TCA supernatants and lysates of sediments were used for determination of IP_X formation and incorporation of radioactivity, respectively, by liquid scintillation counting.

Alternatively, accumulation of IP_X was determined after separation on ion-exchange columns (Dowex 1X8-200, Sigma, USA). In such case cells were harvested by mild trypsinization and resuspenden in Krebs-HEPES buffer (KHB; final concentrations in mM: NaCl 138; KCl 4; $CaCl_2$ 1.3; $MgCl_2$ 1; NaH_2PO_4 1.2; Hepes 20; glucose 10; pH adjusted to 7.4). First, cells were treated with

xanomeline or sham treated: Cells were incubated for 20 min at 37 °C with xanomeline, washed 3 times with KHB, incubated in excess of KHB for 1 h at 37 °C and then washed 3 times with KHB. After treatment, cells were resuspended in KHB supplemented with 500 nM [^{3}H]myo-inositol (ARC, USA) and incubated at 37 °C for 1 h. Then cells were washed once with excess of KHB, resuspended in KHB containing 10 mM LiCl and incubated for 1 h at 37 °C. Incubation was ended by addition of 0.5 mL of stop solution (chloroform:methanol:HCl; 2:1:0.1) and placed on ice for 20 min. An aliquot (0.65 mL) of upper (aqueous) phase was taken and loaded onto ion-exchange columns. Columns were washed with 10 mL of deionized water and 20 mL of 60 mM ammonium formate – 5 mM sodium borate solution. IP_X were collectively eluted from columns by 4 mL of 1 M ammonium formate – 0.1 M formic acid buffer.

2.5. Microfluorometry of intracellular calcium

Cells were washed twice with KHB and then pre-labeled with 5 μM Fura 2-AM in KHB enriched with 1 mM Pluronic® F-68 for one hour at 37 °C. After pre-labeling cells were washed twice with KHB, mounted to a superfusion chamber, placed on a stage of Olympus IX-90 inverted fluorescent microscope, and continuously superfused at a flow rate 0.5 mL/min. Images were recorded using CCD camera connected to a computer equipped with MetaFluor 7.0 software (Visitron Systems GmBH, Germany) for image acquisition and analysis. During the measurements images of the whole visual field containing about 40 cells were saved and analyzed off-line after the measurements. Two pairs of images per second were recorded. Only cells responding to the first (control) carbachol or oxotremorine stimulation were selected (by exclusion of weakly and/or slow responding cells or cells with abnormal response; the outliers in peak value, time to peak or fall time were identified by interquartile range (IQR) where data below Q1 − 1.5*IQR and above Q3 + 1.5*IQR were considered outliers) for further analysis. Calcium signals of selected cells were averaged, normalized to basal calcium level and further analyzed by means of array oriented program Grace [23].

Two general schemes of calcium measurements were employed. In the first scheme dependency of calcium response on the concentration of agonist was measured. Cells expressing wild-type (wt) and mutant M_1 receptors and naive CHO-K1 cells were exposed for 10 s to increasing concentrations of tested agonists (carbachol, oxotremorine, NDMC or xanomeline) separated by 3–6 min perfusion with agonist free KHB medium. In the second scheme, effects of prolonged exposure to xanomeline were tested. Initially, control stimulation with 10 μM oxotremorine lasting 10 s was performed. After 6 min of perfusing with KHB cells were stimulated with 10 μM xanomeline for 40 s. Calcium levels in the absence of xanomeline were measured for the subsequent 6 min.

2.6. Data analysis

Data from experiments were processed in Libre Office and then analyzed and plotted using program Grace [23]. Statistical analysis was performed using statistical package R [24]. For non-linear regression analysis, the following equations were used:

[^{3}H]NMS saturation binding

$$y = B_{MAX} * \frac{x}{x + K_D} \quad (1)$$

where y is specific binding at free concentration x, B_{MAX} is maximum binding capacity, and K_D is equilibrium dissociation constant.

Competition binding

$$y = 100 - (100 - f_{low}) * \frac{x}{x + IC_{50\,high}} - f_{low} * \frac{x}{x + IC_{50\,low}} \quad (2)$$

where y is specific radioligand binding at concentration x of competitor expressed as per cent of binding in the absence of competitor, IC_{50} is concentration causing 50% inhibition of radioligand binding, f_{low} is fraction of low affinity binding sites expressed in per cents. Inhibition constant K_I was calculated as:

$$K_I = \frac{IC_{50}}{1 + [D]/K_D} \quad (3)$$

where $[D]$ is concentration of radioligand used and K_D is its equilibrium dissociation constant.

Concentration response curve

$$y = 1 + (E_{MAX} - 1) * \frac{x^{nH}}{x^{nH} + EC_{50}} \quad (4)$$

where y is response normalized to basal at concentration x, E_{MAX} is maximal effect, EC_{50} is concentration causing half-maximal effect, and nH is Hill coefficient.

To compare efficacies at receptors with different expression level, the apparent affinity constant K_G of the G protein for the agonist-receptor complex was calculated according to Lu and Hulme [25] using the following equation:

$$K_G = \frac{E_{MAX\,FR}}{(1 - E_{MAX\,FR})/B_{MAX}} \quad (5)$$

where $E_{MAX\ FR}$ is maximal response calculated according to Eq. (4) and expressed as a fraction of E_{MAX} of carbachol ($E_{MAX\ agonist} - 1$)/($E_{MAX\ carbachol} - 1$) at M_1 wt CHO cells with high expression and B_{MAX} is maximum binding capacity of cell membranes calculated according to Eq. (1).

2.7. Molecular modeling

2.7.1. Construction of homology models

Homology models of the human M_1 receptor in active and inactive states were constructed using YASARA software [26] as described earlier [27]. For construction of the hM_1 receptor in inactive state structures, 3UON (M_2 receptor with bound antagonist quinuclidinyl bezilate (QNB)) and 4DAJ (M_3 receptor with bound antagonist tiotropium) were used as multiple templates. The resulting homology model of inactive hM_1 receptor contains QNB bound to the orthosteric binding site. For construction of hM_1 receptor in an active state, the structure 4MQS (M_2 receptor in active state stabilized by nanobody and bound agonist iperoxo) was used as a single template. The resulting homology model of an active hM_1 receptor contains iperoxo bound to the orthosteric binding site.

2.7.2. Agonist docking

Docking of agonists was done using Schrodinger Software Suit (Schrödinger LLC, New York, NY). Homology model of the hM_1 receptor in an active state was prepared for docking in Maestro using Protein Preparation Wizard according to Sastry et al. [28] guidelines. Structures of agonists were downloaded from PubChem database (pubchem.ncbi.nlm.nih.gov) and prepared for docking in Maestro using LigPrep. Individual agonists were docked to the receptor using Induced Fit Docking procedure. Iperoxo was set to define the binding site. Size of binding site was increased to contain vestibule at the extracellular edge of transmembrane domain to allow additional binding sites/modes to be identified. Initial Glide docking step was set to “Standard Precision” without explicit constrains. In Prime refinement step amino acid residues within 5 Å form ligand were refined in single pass. Residues N382 and D105 were excluded from refinement. Glide re-docking step was set to “Extra Precision”. For every ligand top 20 poses according to GlideXP score were saved. Top poses were then reevaluated using Prime MM-GB/SA.

2.7.3. Simulation of molecular dynamics

Prime MM-GB/SA top poses were taken for simulation of molecular dynamics. Molecular dynamics was simulated using Desmond/GPU ver. 3.4. The simulated system consisted of receptor–ligand complex in 1-palmitoyl-2-oleoyl-sn-glycero-3-phosphocholine (POPC) membrane set to receptor helices in water and 0.15 NaCl. The system was first relaxed by standard Desmond protocol for membrane proteins and then 1.2 ns NPT (Noose–Hover chain thermostat at 300 K, Martyna–Tobias–Klein barostat at 1.01325 bar, isotropic coupling, Coulombic cutoff at 0.9 nm) followed by 120 ns NVE molecular dynamics without restrains was simulated. In Maestro the quality of molecular dynamics simulation was assessed by Simulation Quality Analysis tools, analyzed by Simulation Event Analysis tool and ligand–receptor interactions were identified using Simulation Interaction Diagram tool.

3. Results

3.1. Effects of mutations on muscarinic ligand binding

Amino acids in the orthosteric binding site (D105), vestibule to binding pocket (D99), activation switch (D71) and receptor-G protein interface (D122 and R123) were mutated (Fig. 1). Binding of the radiolabeled antagonist N-methylscopolamine ([^{3}H]NMS) to membranes from CHO cells expressing wild-type and mutant hM_1 receptor was measured directly in saturation binding experiments. Affinities of [^{3}H]NMS at individual receptors are summarized in Table 1. Mutations D71N, D99N and D105E slightly decreased the affinity for [^{3}H]NMS whereas mutations D122N and R123N had no effect on [^{3}H]NMS binding affinity. Expression level in membranes varied from 3.3 ± 0.4 to 15.8 ± 0.8 fmol of binding sites per μg of protein at R123N and D105E, respectively (Table 2). No specific binding of [^{3}H]NMS was detected at the D105N mutant of hM_1 receptor at radioligand concentrations as high as 10-fold of its K_D. In sharp contrast, the radiolabeled antagonist quinuclidinyl benzilate ([^{3}H]QNB) exhibited maximal binding of 5.8 ± 0.2 fmol binding sites per μg of protein in membranes of cells expressing the D105N mutant, with pK_D of 7.68 ± 0.03, while wild-type hM_1 exhibited 7.9 $\pm$ 0.3 fmol of [^{3}H]QNB binding sites per μg of protein, with pK_D of 9.82 ± 0.02 (means $\pm$ SEM, $n = 3$). According to quantitative RT-PCR, mRNA level of CHO cell line stably transfected with the D105N mutant was the same as mRNA levels of newly generated CHO cell lines expressing mutants (D71N, D99N, D122N and R123N) and wild-type human variant of M_1 receptor.

Affinities of agonists were measured indirectly in competition binding experiments with 1 nM [^{3}H]NMS. Carbachol, oxotremorine, and xanomeline displayed two-site competition binding while NDMC displayed only low affinity binding at the wild-type hM_1 receptor (Fig. 2, Table 1). The proportion of low-affinity binding of oxotremorine and xanomeline was higher than that of carbachol.

In general, mutations D71N, D99N, D105E, D122N and R123N increased the proportion of low-affinity sites with the exception of xanomeline binding at D71N, D99N and D105E, and oxotremorine at D99N and D122N. Mutant D122N bound xanomeline only with low affinity. All agonists bound to the R123N mutant with low affinity.

Mutation D71N increased the affinity of low-affinity binding of carbachol, lowered affinity of low-affinity binding of oxotremorine and had no effect on low-affinity binding of xanomeline and NMDC. In contrast, this mutation increased the affinity of high-affinity binding of oxotremorine and xanomeline. Mutation D99N decreased the affinity of both high- and low-affinity sites for all tested agonists. Mutation D105E increased the affinity of the high-affinity sites for xanomeline while high-affinity binding of carbachol and oxotremorine was not detected at this mutant.

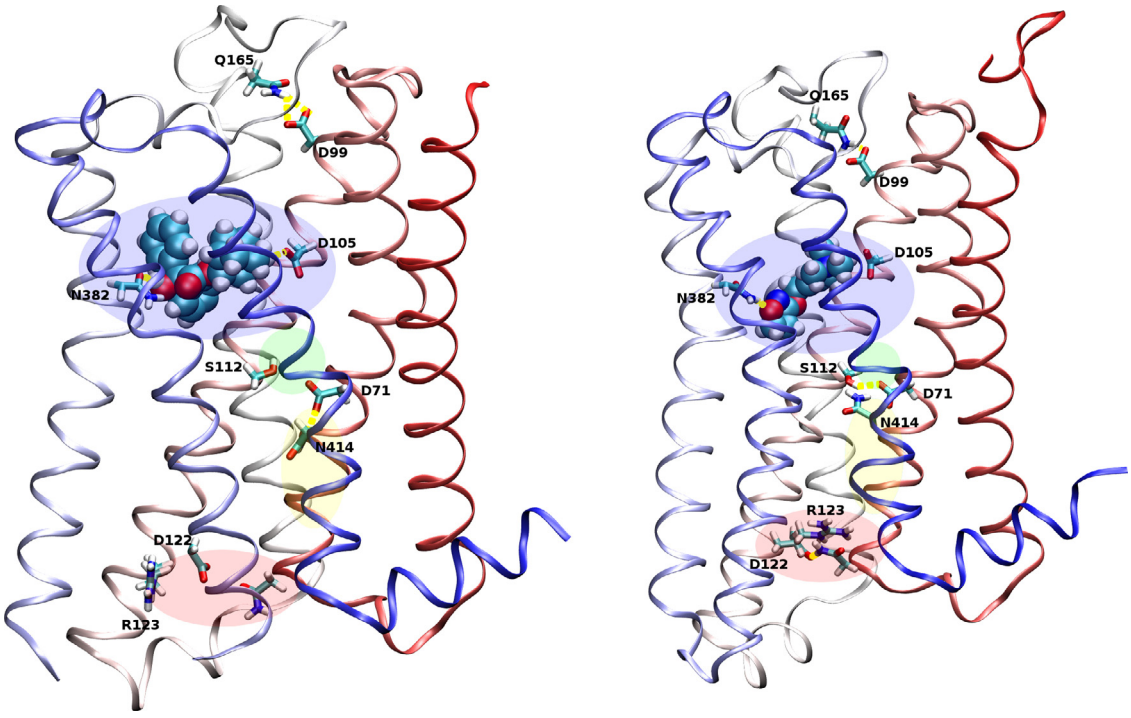

Fig. 1. Amino acids targeted by mutagenesis. Homology models of the hM_1 receptor in an inactive conformation with bound quinuclidinyl benzilate (left) and in an active conformation with bound iperoxo (right). Orientation: extracellular – top, TM VI and VII – front. Backbone of the receptor is colored by position in red to white to blue gradient. Atoms: cyan – receptor carbon, blue – nitrogen, red – oxygen; yellow – hydrogen bonds. D99 forms hydrogen bond with Q165 in o2 loop at both conformations. Domains: blue – orthosteric binding site, green – transmission switch, yellow – tyrosine-toggle switch, red – ionic-lock switch. Both ligands form hydrogen bonds with D105 and N382 in the orthosteric binding site. At inactive conformation D71 forms hydrogen bond with N414 in TM VII that is part of tyrosine-toggle switch. Upon activation it forms hydrogen bond with S112 in TM III. D122 and R123 are free in inactive conformation and form hydrogen bonds with N60 in TM II upon receptor activation.

Table 1
Affinities of muscarinic ligands. Affinities of muscarinic antagonist N-methylscopolamine (NMS) and agonists carbachol, N-desmethylclozapine (NDMC), oxotremorine and xanomline are expressed as negative logarithms of equilibrium dissociation constant K_D (NMS) or inhibition constant K_I (agonists). K_D was obtained by fitting Eq. (1) to the data from saturation experiments. K_Is were computed from IC_{50}s using Eq. (3). IC_{50}s and f_{low}s were obtained by fitting Eq. (2) to the data from competition experiments. Data are means ± S.E.M. from 3 to 8 independent experiments performed in quadruplicates.

	NMS	Carbachol			NDMC	Oxotremorine			Xanomeline		
	pK_D	$pK_{I\ high}$	$pK_{I\ low}$	f_{low}	$pK_{I\ low}$	$pK_{I\ high}$	$pK_{I\ low}$	f_{low}	$pK_{I\ high}$	$pK_{I\ low}$	f_{low}
wt	9.76 ± 0.03	6.45 ± 0.09	3.80 ± 0.04	70 ± 2	7.10 ± 0.02	8.96 ± 0.02	6.04 ± 0.03	83 ± 3[a]	10.12 ± 0.09	7.19 ± 0.04	82 ± 3[a]
D71N	9.29 ± 0.02*	6.49 ± 0.02	4.28 ± 0.04*	85 ± 3*	7.3 ± 0.1	9.7 ± 0.2*	5.50 ± 0.02*	91 ± 2*	10.59 ± 0.02*	7.32 ± 0.04	78 ± 3
D99N	9.41 ± 0.02*	5.7 ± 0.2*	3.31 ± 0.06*	85 ± 1*	6.86 ± 0.04*	8.56 ± 0.01*	5.51 ± 0.08*	86 ± 4	9.2 ± 0.2*	6.4 ± 0.1*	85 ± 4
D105N	n.b.										
D105E	9.15 ± 0.05*	n.c.	2.96 ± 0.03*	100*	6.59 ± 0.04*	n.c.	6.01 ± 0.07	100*	11.36 ± 0.05*	6.50 ± 0.06*	70 ± 4[a]
D122N	9.65 ± 0.05	6.75 ± 0.01*	3.83 ± 0.04	82 ± 1*	6.94 ± 0.09	8.83 ± 0.01	5.83 ± 0.04*	89 ± 2	n.c.	6.85 ± 0.03*	100*
R123N	9.9 ± 0.1	n.c.	3.40 ± 0.1*	100*	7.17 ± 0.02	n.c.	5.80 ± 0.03*	100*	n.c.	6.95 ± 0.01*	100*

n.b., no binding; n.c., not calculated; *, different from wt; [a], f_{low} different from f_{low} of carbachol, $P < 0.05$, ANOVA and Dunnett's post-test

Table 2
Parameters of accumulation inositol phospahtes stimulated by agonists. Half-efficient concentration (EC_{50}) and maximum of stimulation (E_{MAX}) were calculated by fitting Eq. (4) to the data from measurements of inositol phospahtes. Maximum biding capacities (B_{MAX}) were calculated by fitting Eq. (1) to the data from saturation binding experiments and are expressed in pmol per mg of protein. Efficacies (K_G) were calculated from E_{MAX} and B_{MAX} values according to Eq. (5) and data from cell line with high expression of M_1 wt (B_{MAX} = 11.3 ± 0.5; carbachol pEC_{50} = 5.90 ± 0.05; E_{MAX} = 5.2 ± 0.3). Data are means ± S.E.M. from 3 to 8 independent experiments performed in triplicates.

		Carbachol			NDMC			Oxotremorine			Xanomeline		
	B_{MAX}	pEC_{50}	E_{MAX}	K_G	pEC_{50}	E_{MAX}	K_G	pEC_{50}	E_{MAX}	K_G	pEC_{50}	E_{MAX}	K_G
wt	7.6 ± 0.6	6.02 ± 0.04	3.5 ± 0.2	0.19 ± 0.01	6.5 ± 0.2	2.0 ± 0.3[a]	0.041 ± 0.006[a]	6.81 ± 0.08[a]	2.65 ± 0.03[a]	0.085 ± 0.001[a]	7.39 ± 0.09[a]	4.1 ± 0.2[a]	0.37 ± 0.02
D71N	6.9 ± 0.5	n.r.	n.r.	n.r.	n.r.								
D99N	10.6 ± 0.5	5.53 ± 0.08*	2.6 ± 0.2*	0.058 ± 0.004*	6.0 ± 0.1*	1.8 ± 0.2	0.022 ± 0.002*	6.22 ± 0.05*	2.98 ± 0.09*	0.084 ± 0.003	6.92 ± 0.08*	3.9 ± 0.2	0.21 ± 0.01*
D105N	5.8 ± 0.2	n.r.	n.r.	5.8 ± 0.1*	2.4 ± 0.3*	0.086 ± 0.009	n.r.						
D105E	15.8 ± 0.8	3.7 ± 0.1*	2.63 ± 0.03*	0.040 ± 0.01*	5.9 ± 0.2	1.14 ± 0.02*	0.0022 ± 0.0001*	5.73 ± 0.08*	1.35 ± 0.05*	0.0058 ± 0.0002*	5.6 ± 0.1*	1.8 ± 0.1*	0.015 ± 0.001*
D122N	4.1 ± 0.3	5.82 ± 0.03	2.5 ± 0.2*	0.14 ± 0.01	6.33 ± 0.08	1.63 ± 0.07*	0.043 ± 0.002	6.94 ± 0.07	2.7 ± 0.1	0.166 ± 0.006*	7.11 ± 0.09	3.3 ± 0.1*	0.30 ± 0.01
R123N	3.3 ± 0.2	n.r.	n.r.	n.r.	n.r.								

n.r., no response; *, different from wt; [a], different from carbachol at wt, $P < 0.05$ by ANOVA and Dunnett's post-test.

Mutation D122N increased the affinity of high-affinity binding of carbachol and decreased the affinity of low-affinity sites for oxotremorine and xanomeline. Mutation R123N decreased the affinity of low-affinity sites for all agonists except NDMC.

3.2. Effects of mutations on agonist-stimulated accumulation of inositol phosphates

The rank order of potencies in stimulating accumulation of inositol phosphates at the wild-type hM_1 was: xanomeline > oxotremorine ≅ NDMC > carbachol (Fig. 3, Table 2). To compare efficacies at receptors with different expression level the apparent affinity constant K_G of the G protein for the agonist–receptor complex was calculated according to Lu and Hulme [25]. In concert with our previous findings, xanomeline demonstrated twofold higher efficacy than the classical full agonist carbachol [15,16]. Efficacies of NDMC and oxotremorine were 22% and 45% of carbachol efficacy, respectively. None of the tested agonists induced accumulation of inositol phosphates at the D71N or R123N mutants. Mutation D99N decreased potency of all tested agonists about three times. It also decreased the efficacy of all tested agonists except oxotremorine. Only oxotremorine stimulated accumulation of inositol phosphates at the D105N mutant. Efficacy of oxotremorine was the same but potency was 10-times lower than at the wild-type. In contrast, all agonists stimulated accumulation of inositol phosphates at the D105E mutant. Mutation D105E decreased potency of all agonists except NDMC. This mutation caused about twofold decrease in efficacy of NDMC and xanomeline, about fivefold decrease in the efficacy of carbachol and 15-fold decrease in the efficacy of oxotremorine. Mutation D122N had no effect on the potency or efficacy of agonists except an increase in efficacy of oxotremorine.

High concentrations (30 μM and higher) of NDMC decreased accumulation of inositol phosphates in CHO cells expressing D71N, D105N or R123N (mutants that do not show response at lower concentrations of NDMC) (Supplementary Fig. 1). However, the same decrease in accumulation of inositol phosphates was detected in non-transfected CHO-K1 cells. In contrast, high concentrations of xanomeline (≥300 μM) increased accumulation of inositol phosphates in CHO cells expressing D71N, D105N or R123N mutants while 1 mM xanomeline had no effect on accumulation of inositol phosphates in non-transfected CHO-K1 cells (Supplementary File 1).

3.3. Effects of mutations on agonist-evoked release of intracellular calcium

Dependence of intracellular calcium mobilization on the concentration of the agonists carbachol, NDMC, oxotremorine and xanomeline was measured by fluorescent microscopy of FURA-2 in perfused CHO cells expressing D105N, D105E or wild-type hM_1 receptors (Fig. 4). As reported previously, the signal in our system is very stable and independent from extracellular calcium [10]. At wild-type hM_1 receptors the agonists carbachol, oxotremorine and xanomeline produced transient increase in intracellular calcium with a fast rise followed by a slow polyphasic decline (Fig. 4 left column). Time to peak ranged from 6.3 ± 0.3 s for carbachol to 13.1 ± 0.5 s for xanomeline (mean ± S.E.M., $n = 3$). The fall time ranged from 143 ± 6 s for oxotremorine to more than 360 s (length of perfusion after stimulation) for xanomeline. In general, higher concentrations of agonists were needed at D105N to get the same response as at the wild-type hM_1 receptor (Fig. 4 middle column). The rise of intracellular calcium was slower (time to peak was 9.1 ± 0.3 s for carbachol and 16 ± 1 s for xanomeline) but the

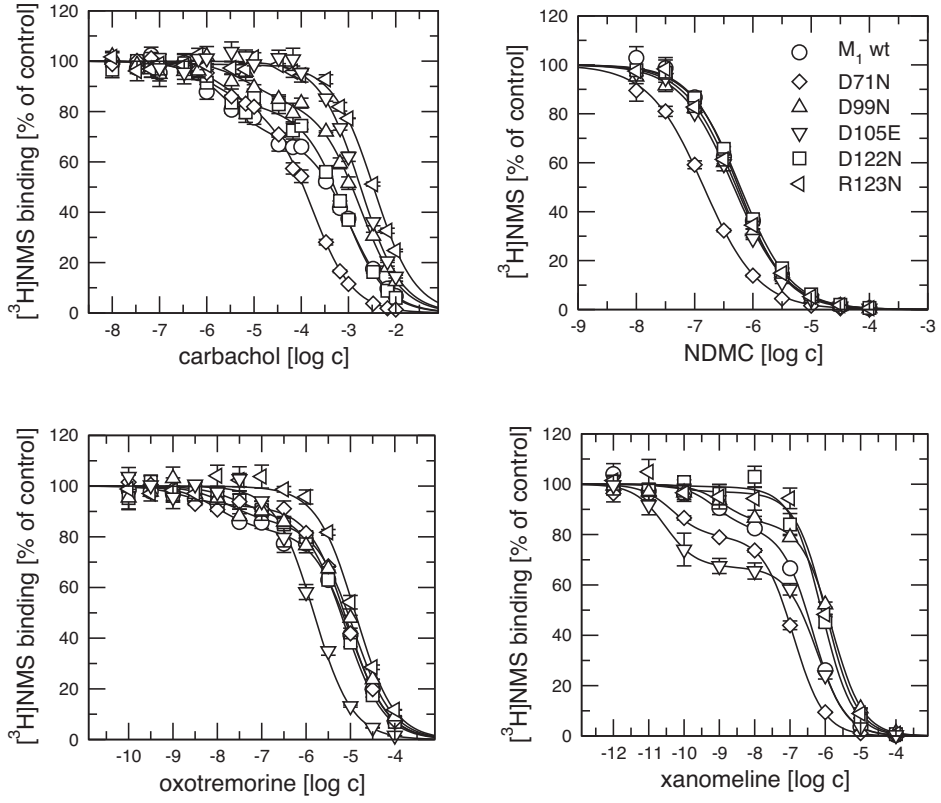

Fig. 2. Competition of agonists with [^{3}H]NMS. Binding of 1 nM [^{3}H]NMS to wild-type (wt) and mutant M_1 receptors in the presence of increasing concentrations of the agonists carbachol (upper left), N-desmethylclozapine (upper right), oxotremorine (lower left) and xanomeline (lower right) is plotted on ordinate as per cent of control binding in the absence of agonists. Data are means ± S.E.M. from 3 to 5 independent experiments performed in quadruplicates. Binding parameters are summarized in Table 1.

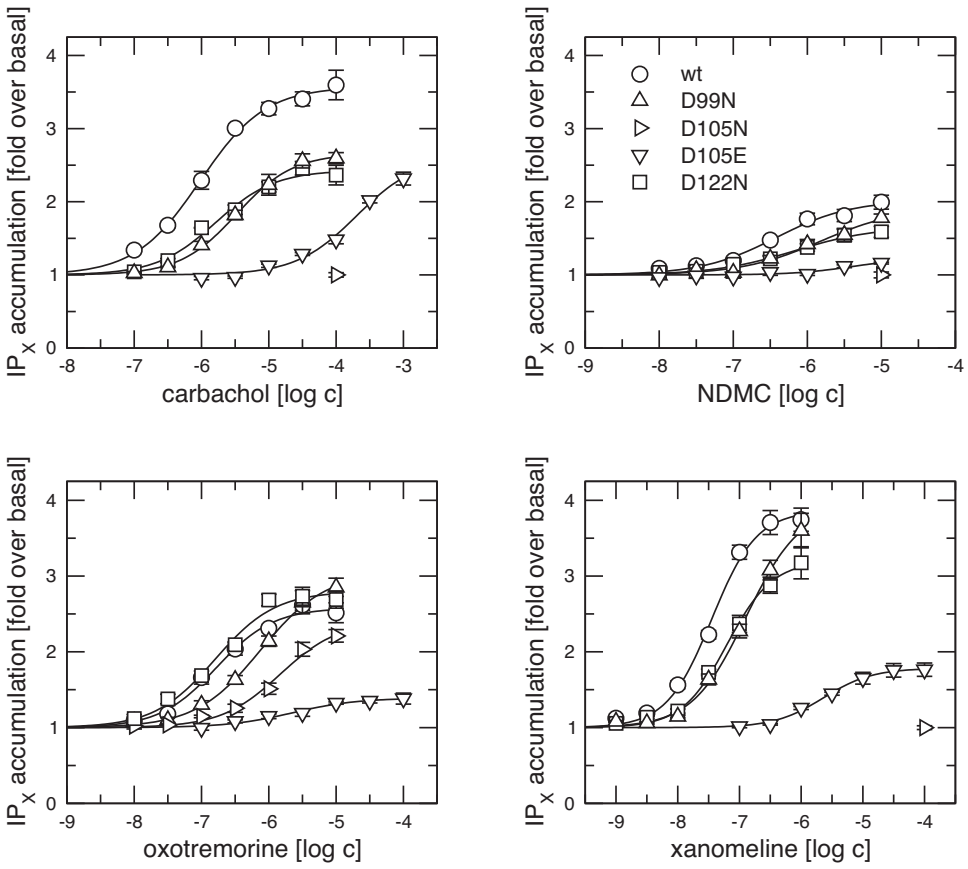

Fig. 3. Effects of agonists on accumulation of inositol phosphates. Accumulation of inositol phosphates in CHO cells expressing wild-type (wt) and mutant M_1 receptors stimulated by increasing concentrations of the agonists carbachol (upper left), N-desmethylclozapine (upper right), oxotremorine (lower left) and xanomeline (lower right) is plotted on ordinate as folds of accumulation under basal conditions without agonists. Data are means ± S.E.M. from 3 to 7 independent experiments performed in triplicates. Binding parameters are summarized in Table 2.

following decline was faster (fall time was 127 ± 6 s for oxotremorine and 320 ± 15 s for xanomeline) than at wild-type hM_1 receptors. In general, the D105E mutation had smaller impact on potency of agonists than D105N. However, its impact on E_{MAX} values was greater than at D105N. The rise times at D105E were even longer and fall times even shorter than at D105N (e.g. for xanomeline the time to peak was 23 ± 2 s and fall time was 250 ± 10 s).

Maximal changes in intracellular calcium concentration (E_{MAX}) from Fig. 4 are plotted against agonist concentration in Fig. 5. The expression level of wild-type M_1 receptor did not affect E_{MAX} of carbachol stimulation. Thus it is not possible to calculate K_G values. Xanomeline was the most potent in increasing intracellular calcium level with pEC_{50} of 7.76 ± 0.04 followed by oxotremorine (7.43 ± 0.04) and carbachol (6.99 ± 0.03) (mean ± S.E.M., $n = 3$). Mutation D105N decreased the potency of all tested agonists. The strongest effect was on the potency of xanomeline, which showed a decrease in potency of almost three thousand fold (to pEC_{50} of 4.3 ± 0.04.) The decrease in potency of carbachol was about one hundred times (to 4.89 ± 0.04) and was less than 10 times for oxotremorine (to 6.50 ± 0.03). Mutation D105N slightly decreased maximal response values of carbachol and xanomeline. The maximal response of oxotremorine remained unchanged. In contrast, mutation D105E decreased the maximal response of carbachol, xanomeline and oxotremorine to 58 ± 3, 36 ± 2 and 24 ± 1% of the value at the wild-type receptor, respectively. In comparison to D105N, at D105E mutant decrease in potency was the same for oxotremorine (about 10-fold) but smaller for carbachol and xanomeline (less than 30-fold).

NDMC increased intracellular calcium levels in non-transfected CHO-K1 cells at concentrations as low as 10 nM and higher (Supplementary File 1) rendering measurements of NDMC action at cells expressing hM_1 receptor variants unfeasible. Thus, this assay was unsuitable for analysis of the effects of D105N mutation on the action of NDMC. None of the tested agonists changed calcium level at the D71N and R123N mutants (data not shown).

3.4. Effects of mutations on extended exposure to xanomeline

In these measurements the effects of mutations D99N, D105N, D105E and D122N on calcium responses evoked by prolonged exposure to xanomeline were estimated. After 10-s initial period, control stimulation with 10 μM oxotremorine was performed for 10 s. Control stimulation was followed by 6-min washing with buffer, 40-s stimulation with 10 μM xanomeline and another 6-min washing with buffer (Fig. 7). In comparison to the wild-type receptor, mutations D99N and D122N had no effect and mutations D105N and D105E decreased the maximal calcium response induced by control oxotremorine stimulation. Exposure of cells expressing the wild-type receptor to 10 μM xanomeline for 40 s led to transient increase (peak of 1.93 ± 0.02; mean ± S.E.M., $n = 3$) in intracellular calcium followed by a plateau (1.31 ± 0.02 of basal). All tested mutations decreased both peak and plateau values compared to wild-type hM_1 receptors ($P < 0.05$, paired t-test). The effect of D99N mutation was the weakest (1.88 ± 0.02 and 1.26 ± 0.02 for peak and plateau values, respectively) and that of D105N mutation was the strongest (1.12 ± 0.02 and 1.03 ± 0.02, respectively). The

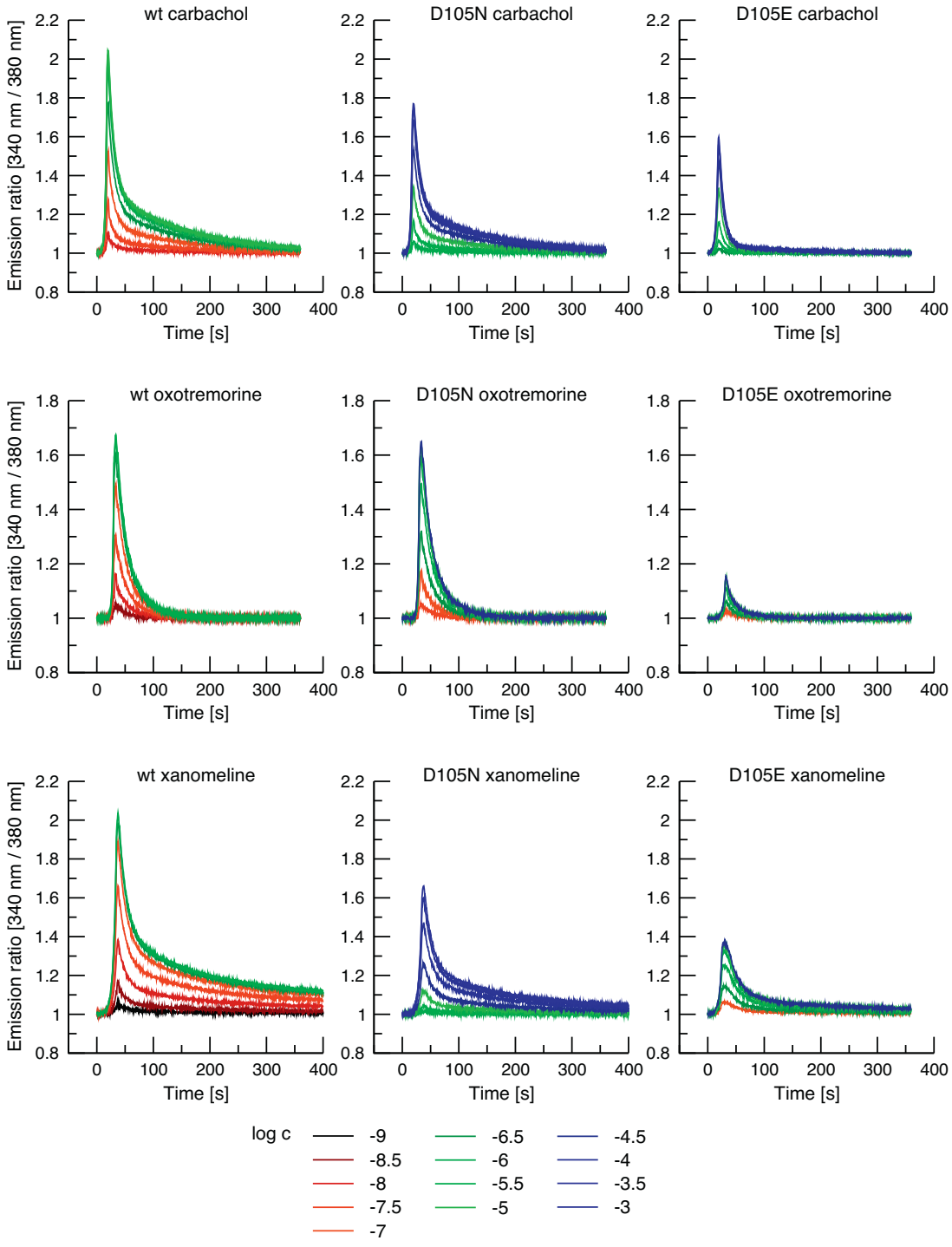

Fig. 4. Time-courses of changes in intracellular calcium level upon exposure of cells to agonists. Time-courses of intracellular calcium of the CHO cells expressing wild-type (left) or D105N (center) and D105E (right) mutants of M_1 receptor upon 10-s exposure to the agonists carbachol (top), oxotremorine (middle) and xanomeline (bottom) at the concentrations indicated in legend are shown. Intacellular calcium level (ordinate) is expressed as 340 nm to 380 nm emission ratio normalized to basal level. Abscissa, time in seconds. Traces are averages from 8 to 12 cells from representative experiment confirmed by 2 additional independent experiments.

plateau at D105N as well as D105E was significantly higher than basal ($P < 0.05$, one-tail t-test).

3.5. *Effects of mutations on xanomeline wash-resistant binding and associated persistent receptor activation*

The apparent affinity of xanomeline wash-resistant binding at wild-type hM_1 receptors was 260 μM. Mutations, except D99N and D105E, had no effect on the apparent affinity of xanomeline wash-resistant binding. Mutation D99N caused about threefold and mutation D105E more than 10-fold decrease in affinity (Table 3). Wash-resistant xanomeline stimulated accumulation of inositol phosphates with half-maximal response at 1 μM. Mutations D71N, D105N and R123N abolished accumulation of inositol phosphates induced by wash-resistant xanomeline. Mutations D99N, D105E and D122N had no effect on the potency of wash-resistant xanomeline. Only mutation D105E caused a twofold decrease in efficacy.

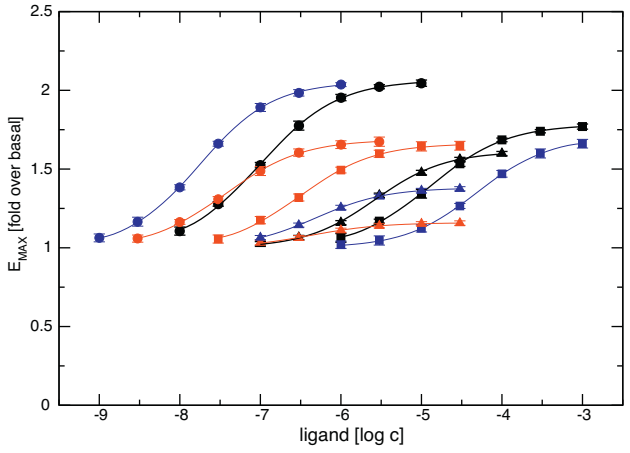

Fig. 5. Concentration dependence of the maximal response of intracellular calcium levels to agonists. Increases in intracellular calcium (ordinate) obtained in experiments as that shown in Fig. 4 in CHO cells expressing wild-type (circles) or D105N (squares) and D105E (triangles) mutants of M_1 receptors upon activation by carbachol (black), oxotremorine (red) and xanomeline (blue) are plotted against used concentration of agonists (abscissa). Data are means ± S.E.M. from 3 independent experiments.

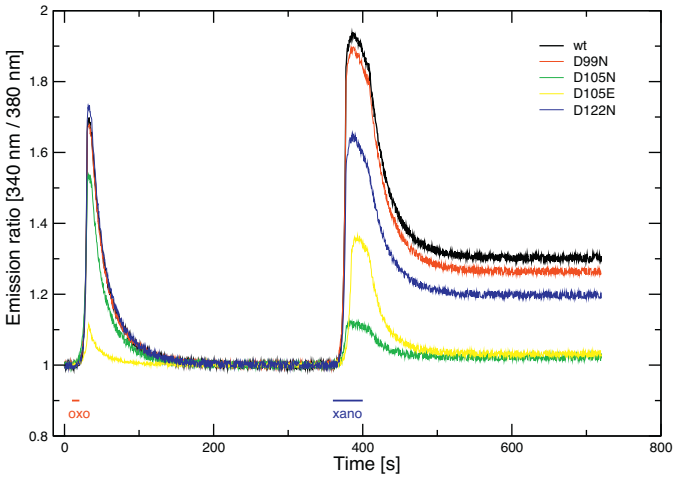

Fig. 6. Time-courses of changes in intracellular calcium level upon prolonged exposure of the cells to xanomeline. Time-courses of intracellular calcium level in CHO cells expressing wild-type (black), or D99N (red), D105N (green), D105E (yellow) and D122N (blue) mutant M_1 receptors are shown. After control 10-s stimulation with 1 μM oxotremorine (oxo) cells were perfused with agonist-free KHB. At the beginning of the seventh min cells were exposed for 40-s to 10 μM xanomeline and then perfused with agonist-free KHB till the end of measurement. Intracellular calcium level (ordinate) is expressed as 340 nm to 380 nm emission ratio normalized to basal level. Traces are averages from 8 to 12 cells from representative experiment confirmed by two additional independent experiments. Abscissa, time in seconds.

3.6. Molecular modeling of agonist binding

The agonists carbachol, NDMC, oxotremorine and xanomeline were docked to the homology model of the hM_1 receptor in an active state. Generated poses were re-scored using Prime MM-GB/SA. Top poses of all tested agonists interact with key amino acids (D105 in TM III and N382 in TM VI) of the orthosteric binding site (Fig. 6). Molecular dynamics (MD) of top poses was simulated. Agonist–receptor interactions were inferred from MD trajectories using Ligand Interaction Diagram in Maestro (Fig. 8). The principal difference found by analysis of ligand receptor interactions over MD trajectory is in interaction of agonists with key amino acids at the orthosteric binding site, namely D105 and N382. The ionizable nitrogen of carbachol, NDMC and xanomeline binds strongly to D105 via ionic bond. Further, the ionizable nitrogen forms hydrogen bonds and water bridges with D105 (NDMC, xanomeline) or Y106 (carbachol). In contrast, oxotremorine binds only weakly to D105 via water bridges. The classical agonists carbachol and oxotremorine form hydrogen bonds and water bridges with N382. As for atypical agonists hydrogen bonding to N382 is much less abundant (NDMC) or negligible (xanomeline). Another marked difference is in the interaction with Y381. While carbachol, oxotremorine and xanomeline exhibit hydrophobic interactions with Y381, the nitrogen in atomic position 4 of NDMC forms a hydrogen bond with this amino acid. Importantly, xanomeline binds to D105 strongly via ionic or hydrogen bonds 100% of the time during MD simulation while carbachol binds to D105 via ionic bond in less than 20% of the time and oxotremorine binds to D105 only weakly via water bridges. Changes in binding energy due to repulsion between N105 in the reverse-charge mutant D105N and agonist nitrogen is much greater than needed for rearrangement of water bridges. Thus, the decrease in affinity and potency is greatest for xanomeline, medium for carbachol and smallest for oxotremorine.

Table 3
Parameters of wash-resistant xanomeline binding and stimulation of accumulation of inositol phosphates. Apparent affinity of xanomeline wash-resistant binding is expressed as negative logarithms of inhibition constant K_I that was computed from IC_{50} using Eq. (3). IC_{50}s and f_{low}s were obtained by fitting Eq. (2) to the data from competition experiments. Data fit to single population of low affinity sites. Half efficient concentration (EC_{50}) and maximum of stimulation (E_{MAX}) were calculated by fitting Eq. (4) to the data from measurements of inositol phosphates. Efficacy (K_G) was calculated from E_{MAX} and B_{MAX} values according to Eq. (5) and data from cell line with high expression of M_1 wt (B_{MAX} = 11.3 ± 0.5; wash-resistant xanomeline pEC_{50} = 6.2 ± 0.1; E_{MAX} = 5.5 ± 0.2). Data are means ± S.E.M. from 3 independent experiments performed in quadruplicates.

	Wash-resistant xanomeline			
	pK_I	pEC_{50}	E_{MAX}	K_G
wt	4.34 ± 0.06	6.0 ± 0.1	3.8 ± 0.3	0.22 ± 0.02
D71N	4.37 ± 0.08		n.r.	
D99N	3.81 ± 0.05*	6.08 ± 0.06	4.3 ± 0.3	0.26 ± 0.02
D105E	3.20 ± 0.1*	6.0 ± 0.1	1.6 ± 0.1	0.010 ± 0.001*
D122N	4.17 ± 0.06	5.9 ± 0.1	2.9 ± 0.1	0.18 ± 0.01
R123N	4.39 ± 0.06		n.r.	

n.r., no response; *, different from wt; $P < 0.05$ by ANOVA and Dunnett's post-test.

4. Discussion

The main finding of this work is that classical as well as atypical agonists activate M_1 muscarinic receptors by the same mechanism involving the D71 activation switch. Further crucial role of the orthosteric binding site in activation by atypical agonists was demonstrated. This is in contrast to studies that suggested that N-desmethylclozapine (NDMC) induces a specific mode of M_1 receptor activation [22] and preferentially activates this receptor by interacting with a site that does not fully overlap with the acetylcholine orthosteric site [21], and other studies that suggested the existence of multiple activation switches specific for allosteric ligands at muscarinic receptors [20]. Several lines of evidence suggest that atypical agonists may induce different receptor conformations and possibly utilize different activation mechanisms at the molecular level. These include differential kinetics of receptor activation by xanomeline [16] (and other agonists [17]) and the existence of agonist-specific conformations of muscarinic receptors [18,19]. To test whether there are principal differences in the action of atypical and classical agonists, we mutated key amino acids of the human variant of the M_1 receptor targeting ligand binding, receptor activation, and receptor-G protein interaction (Fig. 1) and compared effects of these mutations

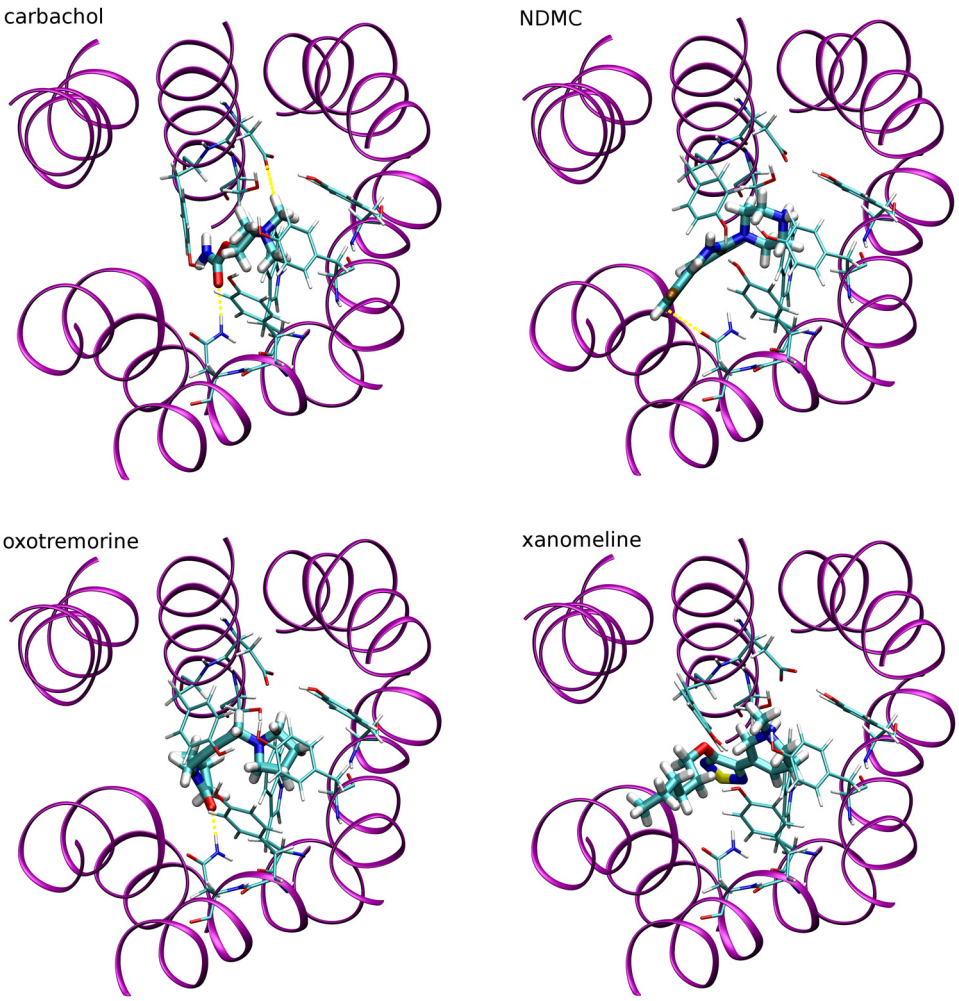

Fig. 7. Top poses of agonists. Top docking poses of carbachol (upper left), NDMC (upper right), oxotremorine (lower left) and xanomeline (lower right) according Prime MM-GB/SA are shown from the extracellular view. Orientation, TM III up and TM VI down. Helices TM II to TM VII are shown in purple. Ligands and displayed amino acids (D105, Y106, S109, W378, Y381, N382 and Y404) are colored according elements: cyan – carbon, white – hydrogen, blue – nitrogen, red – oxygen, yellow – sulfur. Yellow dashed lines denote ligand-receptor hydrogen bonds.

on the action of two atypical M_1 preferring agonists (NDMC and xanomeline) and two classical non-selective orthosteric agonists (the full agonist carbachol and the partial agonist oxotremorine).

Aspartate in the middle of TM III ($D^{3.32}$, numbering according Ballesteros and Weinstein [29]) is conserved among aminergic GPCRs (subclass A17 through A19) and is essential for ligand binding. Opsin receptors (subclass A16) have glutamate in this position that interacts with opsins. On the other hand, chemokine receptors have basic amino acids in this position. $D^{3.32}$ of muscarinic receptors (D105 in the hM_1 sequence; Fig. 1) has been identified to be essential for binding of classical muscarinic agonists and antagonists and it has been proven that it interacts with the positively charged nitrogen moiety of muscarinic ligands [30,31]. Mutation of D105 to asparagine completely ablated binding of the tritiated antagonist N-methylscopolamine ([^{3}H]NMS) (Table 1) and decreased the affinity of quinuclidinyl benzilate more than 100-times. Deteriorating effects of D105N and D105E mutations on binding were projected to functional assays (Fig. 3, Table 2). Surprisingly, the mutations D105N and D105E in the orthosteric binding site decreased potency of xanomeline (an atypical agonist with allosteric properties) more than the potency of carbachol and oxotremorine (classical agonists believed to bind primarily to the orthosteric binding site) (Figs. 4 and 5).

Effects of mutations of D105 on ligand binding may be explained by molecular modeling that shows that while all tested agonists bind to the orthosteric binding site (Fig. 7), agonists differ in the way they interact with individual amino acids within this site, especially D105 (Fig. 8). This is in accordance with current findings [32]. Specifically, xanomeline binds to D105 strongly via ionic or hydrogen bonds 100% of the time during MD simulation. Carbachol binds to D105 via ionic bond in less than 20% of the time of MD simulation. Oxotremorine binds to D105 only weakly via water bridges. Change in binding energy due to repulsion between N105 in the reverse-charge mutant D105N and agonist's charged quaternary nitrogen is much greater than the change in binding energy due to rearrangement of water bridges. Thus, the decrease in affinity and potency is greatest for xanomeline, medium for carbachol and smallest for oxotremorine. Analogously, affinity of antagonist containing charged quaternary nitrogen (NMS) is affected more than affinity of antagonist containing ternary nitrogen (QNB). Conserved mutant D105E only changes geometry of the orthosteric binding site. Thus its effects on agonist affinity and potency are smaller in comparison to the reverse-charge mutant D105N. Thanks to flexibility of oxotremorine binding to E105 via water bridges, affinity of this agonist is not affected by the D105E mutation (Table 1). However, proper conformational change upon agonist binding is a

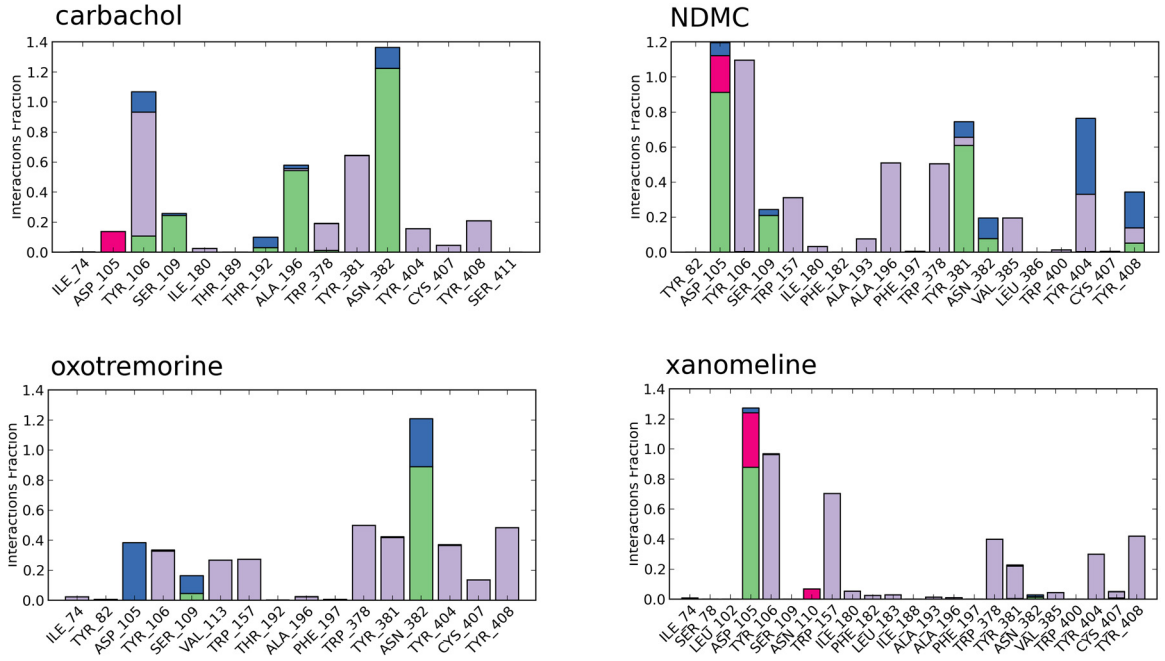

Fig. 8. Interaction of agonists with receptor. Histograms of carbachol (upper left), NDMC (upper right), oxotremorine (lower left) and xanomeline (lower right) interactions with the receptor were calculated from MD trajectories using Ligand Interaction Diagram in Maestro. Ligand-receptor interactions are categorized into four types: Hydrogen bonds (green), hydrophobic (purple), ionic (red) and water bridges (blue). The stacked bar charts are normalized over the course of the trajectory. Values over 1.0 are possible as some protein residues may make multiple contacts of the same type with the ligand within one time-frame.

prerequisite for receptor activation and thus oxotremorine potency is severely affected by this mutation (Table 2).

Aspartate at the junction of the third transmembrane helix (TM III) and the second extracellular (o2) loop $D^{3.26}$ (D99 in the hM_1 sequence; Fig. 1) is not conserved among GPCRs. Adrenergic receptors have glutamate in this position and mutation of this glutamate to alanine had no effects on affinity of agonists and antagonists [33]. However it has been shown that mutation of D99 at M_1 muscarinic receptors decreases affinity and accelerates kinetics of binding of muscarinic ligands [34,35]. A tandem two-site binding model for muscarinic ligands was proposed to explain the role of this aspartate [36]. The model was confirmed by simulation of molecular dynamics of ligand binding to M_2 and M_3 receptors that showed metastable binding state in the extracellular domain (vestibule to the orthosteric site) [6]. Mutation of this aspartate (D99N) decreased the affinity of the antagonist NMS as well as all tested agonists (Table 1). The decrease in agonist affinity was translated as decreased potency of all agonists in functional assays (Table 2). Taken together both D105 within the orthosteric binding site as well as D99 out of the orthosteric binding site participate in binding of all tested agonists.

Network transducing conformational change upon ligand binding that is common among aminergic GPCRs includes a "transmission switch" (WXP motif in TM VI), a "tyrosine-toggle switch" (NPXXY motif in TM VII) and "ionic-lock switch" (DRY motif in TM III interacting with glutamate 6.30) [37,38] (Fig. 1). The aspartate $D^{2.50}$ in the middle of TM II is conserved throughout GPCRs and its reverse-charge mutation to asparagine ablates functional response of many GPCRs including serotonin, adrenergic, cannabinoid, thyrotropin-releasing hormone, etc. (GPCR database; www.gpcr.org/7tm). Specifically, $D^{2.50}$ of muscarinic receptors (D71 in the hM_1 sequence) interacts with $N^{7.49}$ (N414 in the hM_1 sequence) in tyrosine-toggle switch and transfers the conformational change upon agonist binding to the receptor-G protein interface [38,39]. Additional mechanisms of receptor activation were identified among Class A of GPCRs [40–43] including muscarinic receptors [20]. Interestingly, irreversible agonist of β_2-adrenergic receptors activates them through an activation switch that contains $I^{3.40}$, $P^{5.50}$ and $F^{6.44}$ [44] and is parallel to the common network of activation switches. However, mutation D71N completely abolished the ability of all tested agonists to activate the receptor (Table 2; Fig. 3) and renders the possibility that tested atypical agonists utilize activation mechanisms that parallel common activation network unlikely. Thus, atypical agonists activate the hM_1 receptor by the same molecular switch as classical agonists.

Arginine $R^{3.50}$ at the intracellular end of TM III is conserved within all GPCRs. It has been shown to interact directly with the α-subunit of G-proteins [45]. Although in the majority of cases, mutation of $R^{3.50}$ leads to complete loss of functional response to agonists (GPCR database; www.gpcr.org/7tm/mutant), non-conservative mutations of this amino acid do not abolish signaling via G-proteins in some cases [46,47]. In accordance with previous findings [34], mutation of $R^{3.50}$ (R123N) completely abolished the ability of carbachol to activate the receptor as it failed to stimulate accumulation of inositol phosphates (Table 2) and release of calcium from intracellular stores. This mutation also abolished the functional response to tested atypical agonists. Unlike the D71N mutation, R123N decreased the affinity of agonists at the low-affinity binding site (Table 1, Fig. 2 left triangles), demonstrating that inactive (D71N) and un-coupled (R123N) represent different states of the receptor [48].

The role of the aspartate/glutamate in the conserved E/DRY motif (position 3.49) is to stabilize the interaction of TM III and TM VI of the inactive receptor and thus stabilizes the inactive conformation of the receptor [49]. Similar to adrenergic [50] and 5-hydroxytryptamine [51] receptors, mutation of $D^{3.49}$ to asparagine (D122N) in muscarinic receptors results in an increase in receptor constitutive activity [18] by destabilization of the inactive conformation. The most profound effect of D122N was an increase in the proportion of low-affinity binding sites (Table 1, Fig. 2 squares). The increase in low-affinity sites is probably a consequence of increased basal activity of the receptor.

Part of xanomeline binding is resistant to washing and leads to long-term receptor activation [7]. Exposure of the wild-type hM_1 to a high concentration of xanomeline led to sustained activation (Fig. 6, black trace). The ratio between peak and plateau levels of intracellular calcium at D105N and D105E is similar to that at the wild-type receptor, indicating that xanomeline binding to the orthosteric binding site is a prerequisite for formation of xanomeline wash-resistant binding and activation. The apparent equilibrium dissociation constant of xanomeline wash-resistant binding is the same for wild-type and mutants with the exception of a decrease at D105E (Table 3). Also only D105E among functional mutants decreased the efficacy of wash-resistant xanomeline to stimulate accumulation of inositol phosphates. These data suggest the importance of D105 in the orthosteric binding site for long-term activation by wash-resistant xanomeline. This is in concert with the finding that blocking of the orthosteric site by the antagonist NMS transiently diminishes activation of muscarinic receptors by wash-resistant xanomeline [15].

In summary, our data show that the principal difference between classical and atypical agonists is in the way they interact with the orthosteric binding site. However, the atypical agonists NDMC and xanomeline activate M_1 muscarinic receptor via the same molecular switch as the classical agonists carbachol and oxotremorine that involves D71 in TM II. Data also demonstrate a key role of the orthosteric binding site in long-term receptor activation by wash-resistant xanomeline.

Acknowledgments

This work was supported by the Czech Academy of Sciences project [AV0Z 50110509] and institutional support [RVO:67985823], the Grant Agency of the Czech Republic grants [305/09/0681] and [P304/12/G069] and Ministry of Education, Youth and Sports program [OPVK CZ.1.07/2.3.00/30.0025].

Appendix A. Supplementary data

Supplementary data associated with this article can be found, in the online version, at http://dx.doi.org/10.1016/j.phrs.2015.04.002

References

[1] R.M. Eglen, Overview of muscarinic receptor subtypes, Handb. Exp. Pharmacol. (2012) 3–28.
[2] C.J. Langmead, J. Watson, C. Reavill, Muscarinic acetylcholine receptors as CNS drug targets, Pharmacol. Ther. 117 (2008) 232–243.
[3] A. Fisher, Cholinergic modulation of amyloid precursor protein processing with emphasis on M1 muscarinic receptor: perspectives and challenges in treatment of Alzheimer's disease, J. Neurochem. 120 (Suppl. 1) (2012) 22–33.
[4] C.K. Jones, N. Byun, M. Bubser, Muscarinic and nicotinic acetylcholine receptor agonists and allosteric modulators for the treatment of schizophrenia, Neuropsychopharmacology 37 (2012) 16–42.
[5] K. Haga, A.C. Kruse, H. Asada, T. Yurugi-Kobayashi, M. Shiroishi, et al., Structure of the human M2 muscarinic acetylcholine receptor bound to an antagonist, Nature 482 (2012) 547–551.
[6] A.C. Kruse, J. Hu, A.C. Pan, D.H. Arlow, D.M. Rosenbaum, et al., Structure and dynamics of the M3 muscarinic acetylcholine receptor, Nature 482 (2012) 552–556.
[7] A. Christopoulos, T.L. Pierce, J.L. Sorman, E.E. El-Fakahany, On the unique binding and activating properties of xanomeline at the M1 muscarinic acetylcholine receptor, Mol. Pharmacol. 53 (1998) 1120–1130.
[8] T.A. Spalding, C. Trotter, N. Skjaerbaek, T.L. Messier, E.A. Currier, et al., Discovery of an ectopic activation site on the M(1) muscarinic receptor, Mol. Pharmacol. 61 (2002) 1297–1302.
[9] C.K. Jones, A.E. Brady, A.A. Davis, Z. Xiang, M. Bubser, et al., Novel selective allosteric activator of the M1 muscarinic acetylcholine receptor regulates amyloid processing and produces antipsychotic-like activity in rats, J. Neurosci. 28 (2008) 10422–10433.
[10] L.T. May, V.A. Avlani, C.J. Langmead, H.J. Herdon, M.D. Wood, et al., Structure-function studies of allosteric agonism at M2 muscarinic acetylcholine receptors, Mol. Pharmacol. 72 (2007) 463–476.
[11] W. Si, X. Zhang, Y. Niu, H. Yu, X. Lei, et al., A novel derivative of xanomeline improves fear cognition in aged mice, Neurosci. Lett. 473 (2010) 115–119.
[12] A. Bonifazi, H. Yano, F. Del Bello, A. Farande, W. Quaglia, et al., Synthesis and biological evaluation of a novel series of heterobivalent muscarinic ligands based on xanomeline and 1-[3-(4-butylpiperidin-1-yl)propyl]-1,2,3,4-tetrahydroquinolin-2-one (77-LH-28-1), J. Med. Chem. 57 (2014) 9065–9077.
[13] J. Jakubík, S. Tucek, E.E. El-Fakahany, Allosteric modulation by persistent binding of xanomeline of the interaction of competitive ligands with the M1 muscarinic acetylcholine receptor, J. Pharmacol. Exp. Ther. 301 (2002) 1033–1041.
[14] M.K.O. Grant, E.E. El-Fakahany, Persistent binding and functional antagonism by xanomeline at the muscarinic M5 receptor, J. Pharmacol. Exp. Ther. 315 (2005) 313–319.
[15] E. Santrůčková, V. Doležal, E.E. El-Fakahany, J. Jakubík, Long-term activation upon brief exposure to xanomleline is unique to M1 and M4 subtypes of muscarinic acetylcholine receptors, PLOS ONE 9 (2014) e88910.
[16] J. Jakubík, E.E. El-Fakahany, V. Dolezal, Differences in kinetics of xanomeline binding and selectivity of activation of G proteins at M(1) and M(2) muscarinic acetylcholine receptors, Mol. Pharmacol. 70 (2006) 656–666.
[17] N. Ziegler, J. Bätz, U. Zabel, M.J. Lohse, C. Hoffmann, FRET-based sensors for the human M1-, M3-, and M5-acetylcholine receptors, Bioorg. Med. Chem. 19 (2011) 1048–1054.
[18] J. Jakubík, H. Janíčková, E.E. El-Fakahany, V. Doležal, Negative cooperativity in binding of muscarinic receptor agonists and GDP as a measure of agonist efficacy, Br. J. Pharmacol. 162 (2011) 1029–1044.
[19] R.A. Navarro-Polanco, E.G. Moreno Galindo, T. Ferrer-Villada, M. Arias, J.R. Rigby, et al., Conformational changes in the M2 muscarinic receptor induced by membrane voltage and agonist binding, J. Physiol. 589 (2011) 1741–1753.
[20] V. Nawaratne, K. Leach, C.C. Felder, P.M. Sexton, A. Christopoulos, Structural determinants of allosteric agonism and modulation at the M4 muscarinic acetylcholine receptor: identification of ligand-specific and global activation mechanisms, J. Biol. Chem. 285 (2010) 19012–19021.
[21] C. Sur, P.J. Mallorga, M. Wittmann, M.A. Jacobson, D. Pascarella, et al., N-desmethylclozapine, an allosteric agonist at muscarinic 1 receptor, potentiates N-methyl-D-aspartate receptor activity, Proc. Natl. Acad. Sci. U. S. A. 100 (2003) 13674–13679.
[22] T.A. Spalding, E.S. Burstein, Constitutive activity of muscarinic acetylcholine receptors, J. Recept. Signal Transduct. Res. 26 (2006) 61–85.
[23] Grace Development Team Grace: A plotting tool, 2014. Grace Development Team. http://hplasma-gate.weizmann.ac.il/Grace/
[24] R Core Team R, A Language and Environment for Statistical Computing, R Foundation for Statistical Computing, Vienna, Austria, 2014 http://www.R-project.org
[25] Z.L. Lu, E.C. Hulme, The functional topography of transmembrane domain 3 of the M1 muscarinic acetylcholine receptor, revealed by scanning mutagenesis, J. Biol. Chem. 274 (1999) 7309–7315.
[26] E. Krieger, G. Koraimann, G. Vriend, Increasing the precision of comparative models with YASARA NOVA – a self-parameterizing force field, Proteins 47 (2002) 393–402.
[27] J. Jakubík, A. Randáková, V. Doležal, On homology modeling of the M2 muscarinic acetylcholine receptor subtype, J. Comput. Aided Mol. Des. 27 (2013) 525–538.
[28] G.M. Sastry, M. Adzhigirey, T. Day, R. Annabhimoju, W. Sherman, Protein and ligand preparation: parameters, protocols, and influence on virtual screening enrichments, J. Comput. Aided Mol. Des. 27 (2013) 221–234.
[29] J. Ballesteros, H. Weinstein, in: S. Sealfon, P. Conn (Eds.), Methods in Neurosciences, Academic Press, San Diego, CA, 1995.
[30] N.J. Birdsall, A.S. Burgen, E.C. Hulme, A study of the muscarinic receptor by gel electrophoresis, Br. J. Pharmacol. 66 (1979) 337–342.
[31] T.A. Spalding, N.J. Birdsall, C.A. Curtis, E.C. Hulme, Acetylcholine mustard labels the binding site aspartate in muscarinic acetylcholine receptors, J. Biol. Chem. 269 (1994) 4092–4097.
[32] P. Keov, L. López, S.M. Devine, C. Valant, J.R. Lane, et al., Molecular mechanisms of bitopic ligand engagement with the M1 muscarinic acetylcholine receptor, J. Biol. Chem. 289 (2014) 23817–23837.
[33] C.D. Strader, I.S. Sigal, R.B. Register, M.R. Candelore, E. Rands, et al., Identification of residues required for ligand binding to the beta-adrenergic receptor, Proc. Natl. Acad. Sci. U. S. A. 84 (1987) 4384–4388.
[34] C.M. Fraser, C.D. Wang, D.A. Robinson, J.D. Gocayne, J.C. Venter, Site-directed mutagenesis of m1 muscarinic acetylcholine receptors: conserved aspartic acids play important roles in receptor function, Mol. Pharmacol. 36 (1989) 840–847.
[35] J.A. Goodwin, E.C. Hulme, C.J. Langmead, B.G. Tehan, Roof and floor of the muscarinic binding pocket: variations in the binding modes of orthosteric ligands, Mol. Pharmacol. 72 (2007) 1484–1496.
[36] J. Jakubík, E.E. El-Fakahany, S. Tuček, Evidence for a tandem two-site model of ligand binding to muscarinic acetylcholine receptors, J. Biol. Chem. 275 (2000) 18836–18844.
[37] B. Trzaskowski, D. Latek, S. Yuan, U. Ghoshdastider, A. Debinski, et al., Action of molecular switches in GPCRs – theoretical and experimental studies, Curr. Med. Chem. 19 (2012) 1090–1109.
[38] E.C. Hulme, GPCR activation: a mutagenic spotlight on crystal structures, Trends Pharmacol. Sci. 34 (2013) 67–84.
[39] Y. Miao, S.E. Nichols, P.M. Gasper, V.T. Metzger, J.A. McCammon, Activation and dynamic network of the M2 muscarinic receptor, Proc. Natl. Acad. Sci. U. S. A. 110 (2013) 10982–10987.

[40] S. Chen, F. Lin, M. Xu, R.M. Graham, Phe(303) in TMVI of the alpha(1B)-adrenergic receptor is a key residue coupling TM helical movements to G-protein activation, Biochemistry 41 (2002) 588–596.
[41] I. Nachtergael, N. Gaspard, C. Langlet, P. Robberecht, I. Langer, Asn229 in the third helix of VPAC1 receptor is essential for receptor activation but not for receptor phosphorylation and internalization: comparison with Asn216 in VPAC2 receptor, Cell. Signal. 18 (2006) 2121–2130.
[42] N. Singh, S.P. Pydi, J. Upadhyaya, P. Chelikani, Structural basis of activation of bitter taste receptor T2R1 and comparison with Class A G-protein-coupled receptors (GPCRs), J. Biol. Chem. 286 (2011) 36032–36041.
[43] C.E. Scott, R. Abrol, K.H. Ahn, D.A. Kendall, W.A3. Goddard, Molecular basis for dramatic changes in cannabinoid CB1 G protein-coupled receptor activation upon single and double point mutations, Protein Sci. 22 (2013) 101–113.
[44] D.M. Rosenbaum, C. Zhang, J.A. Lyons, R. Holl, D. Aragao, et al., Structure and function of an irreversible agonist-β(2) adrenoceptor complex, Nature 469 (2011) 236–240.
[45] P. Scheerer, J.H. Park, P.W. Hildebrand, Y.J. Kim, N. Krauss, et al., Crystal structure of opsin in its G-protein-interacting conformation, Nature 455 (2008) 497–502.
[46] J. Roland, B.J. Murphy, B. Ahr, V. Robert-Hebmann, V. Delauzun, et al., Role of the intracellular domains of CXCR4 in SDF-1-mediated signaling, Blood 101 (2003) 399–406.
[47] H. Römpler, H. Yu, A. Arnold, A. Orth, T. Schöneberg, Functional consequences of naturally occurring DRY motif variants in the mammalian chemoattractant receptor GPR33, Genomics 87 (2006) 724–732.
[48] J. Jakubík, H. Janíčková, A. Randáková, E.E. El-Fakahany, V. Doležal, Subtype differences in pre-coupling of muscarinic acetylcholine receptors, PLOS ONE 6 (2011) e27732.
[49] T. Okada, M. Sugihara, A. Bondar, M. Elstner, P. Entel, et al., The retinal conformation and its environment in rhodopsin in light of a new 2.2 A crystal structure, J. Mol. Biol. 342 (2004) 571–583.
[50] A. Scheer, F. Fanelli, T. Costa, P.G. De Benedetti, S. Cotecchia, Constitutively active mutants of the alpha 1B-adrenergic receptor: role of highly conserved polar amino acids in receptor activation, EMBO J. 15 (1996) 3566–3578.
[51] C.D. Wang, T.K. Gallaher, J.C. Shih, Site-directed mutagenesis of the serotonin 5-hydroxytrypamine2 receptor: identification of amino acids necessary for ligand binding and receptor activation, Mol. Pharmacol. 43 (1993) 931–940.